Journal of
Engineering Sciences
Faculty of Engineering
Assiut University
JES
مجلة
العلوم الهندسية
كلية الهندسة
جامعة أسيوط
journal homepage: http://jesaun.journals.ekb.eg

Performance of a Robust Passivity-Fuzzy Logic Controller for a Doubly Fed Induction Generator

Received 18 July; Revised 06 September 2025; Accepted 06 September 2025

Izzeddine Allali [1]
Abdelber Bendaoud [2]
Boubekeur Dehiba [3]

Keywords
Doubly fed induction generator, Wind power, Passivity-based control, IT2-FLC , IDA-PBC.

Abstract*:* The article discussed a robust control strategy that combined passivity with interval type-2 fuzzy logic for a wind energy conversion system (WECS) using a variable speed wind turbine (WT) and a doubly fed induction generator (DFIG). The main objective was to optimize active and reactive power flow from the generator to the grid while maintaining stable operation, with rotor signals regulated by a bidirectional converter. This approach effectively managed high uncertainty in complex, nonlinear systems by merging interconnection and damping assignment (IDA) passivity-based control (PBC) with interval type-2 fuzzy logic control (IT2-FLC). The IDA-PBC method compensated for nonlinear characteristics without eliminating them, while IT2-FLC improved how uncertainties were handled by addressing vagueness and unreliable information. A comprehensive comparison with passivity-based control (PBC) was conducted, and the proposed methods were evaluated under various conditions, including speed fluctuations and parameter variations. simulation results indicate that the proposed passivity-fuzzy logic Controller (PFLC) significantly outperforms IDA-PBC strategies in terms of rise time, reference tracking accuracy, error minimization, overshoot, and power ripple. Furthermore, the PFLC achieves a reduction in total harmonic distortion (THD) by 8.35% and 6.61% in two separate tests relative to the IDA-PBC approach. The integration of IDA-PBC and IT2-FLC enhanced the system's dynamic performance by reducing sensitivity to disturbances and improving its ability to manage parameter changes, resulting in greater stability and robustness under varying conditions.

1. Introduction

Over the past decade, the wind energy sector has experienced substantial and sustained growth, primarily due to its environmental sustainability, economic viability, and technological advancements [1, 2, 3]. As conventional fuel reserves diminish, the costs of traditional power generation methods

[1] IRECOM Laboratory, Faculty of Electrical Engineering , Djilali Liabès University of Sidi Bel-Abbès, Algeria, izzeddine.allali@univ-sba.dz
[2] APELEC Laboratory, Faculty of Electrical Engineering, Djilali Liabès University of Sidi Bel-Abbès, Algeria abdelber.bendaoud@univ-sba.dz
[3] IRECOM Laboratory, Faculty of Electrical Engineering , Djilali Liabès University of Sidi Bel-Abbès, Algeria, deh_mas@yahoo.fr

https://doi.org/ 10.21608/jesaun.2025.405271.1622
This is an open access article under the CC BY-NC-ND license (http://creativecommons.org/licenses/by-nc-nd/4.0/).

have increased. At the same time, worries about global warming and running out of fossil fuel supplies have made wind energy stand out as a top renewable energy option. In line with this trend, there was a 54% increase in new wind energy installations in 2023 compared to the previous year. This growth translated into an additional 117 gigawatts of capacity, raising the total global cumulative wind energy capacity to 1 terawatt [4].

Doubly fed induction generators (DFIGs) are commonly used in electricity generation due to their ease of installation, can control their own active and reactive power (Ps and Qs), and can run at different speeds (within 30% of synchronous speed). They are known for their low maintenance requirements, improved power quality, and low cost [5,6]. Two inverters control their rotor voltage, providing precise power regulation that sets them apart from other generators, especially in conditions with variable wind speed (WS) [7]. The DFIG is susceptible to a number of limitations, such as parameter uncertainties (temperature, saturation, and so on) and speed variation disturbances, both of which have the potential to undermine its ideal performance [8,9]. Consequently, it is essential to devise a control method that ensures both resilience and performance. A comprehensive awareness of the system's characteristics and the capacity to react appropriately are essential for effective deployment. The interconnectedness of the system variables complicates the approach for regulating the system [9,10].

Nonlinear techniques such as sliding mode [11], Fuzzy Sliding Mode control [8], SIDA-PBC [12], and fuzzy logic [13] can address this problem. The main disadvantage of these approaches is their dependence on a strict mathematical framework. Conversely, strategies like passive control provide alternatives that are more grounded in physical interpretation [14].

Energy is the main element in passive-based control (PBC) of electrical engineering systems. The transient and steady-state behavior of a system is governed by its energy function, which is achieved through energy transfer among its subsystems. Therefore, systems (processes and controllers) are considered energy-transforming devices that are interconnected to achieve the desired behavior by incorporating prior knowledge and providing the necessary control modes [15].

Ortega and Spong came up with passivity-based control (PBC) in 1989 [16]. They designed a controller that used the concept of passivity to stabilize systems. This controller design had two main purposes. First, it aimed to ensure that the passive system had the least amount of stored energy possible when it reached the desired equilibrium point. This ensured that, at equilibrium, the system's energy storage would be at its lowest possible level. Second, the controller guaranteed asymptotic stability in the passive system's output, meaning that, over time, the output would reliably converge to the equilibrium point without oscillating or diverging. This approach drew inspiration from the stability characteristics inherent in mechanical systems, described mathematically by Euler-Lagrange equations [15].

PBC is also widely used for electrical and electromechanical physical systems [12, 17, 18]. PBC focuses on improving energy reintegration through feedback to enhance natural dissipation. Interconnection and Damping Assignment (IDA) stabilizes the system at desired equilibria by reconfiguring energy and adding damping for convergence. Fuzzy control (FL) is the predominant use of FL in managing complicated nonlinear systems. The methodology used is grounded on the universal approximation feature of fuzzy systems. This fuzzy control methodology seeks to resolve process control issues that are challenging to automate with traditional methods or where the information sources are deemed inaccurate or uncertain, relying on the expertise of knowledgeable operators engaged in the process. The distinctive feature of this control lies in its capacity to emulate

human behavior rather than constructing a mathematical model of the system. This enables the fuzzy controller to operate as an algorithm that converts a formal control strategy, grounded in expert knowledge, into an automated control strategy. This control technique relies on a compilation of fuzzy rules known as a rule base. All control rules are interconnected via the principles of implication, fuzzy composition, and fuzzy inference rules.

In 1965, Professor Zadeh established fuzzy theory by regulating a boiler and steam engine by linguistic rules utilizing the Mamdani fuzzy inference technique [13]. Recent research has concentrated on type-2 fuzzy logic systems (T2FLS), as described by L. Zadeh, which mitigate the shortcomings of type-1 fuzzy logic systems (T1FLS) in managing uncertainties and nonlinearities [18,19,20]. T2FLS employs the Footprint of Uncertainty (FOU) to proficiently address these difficulties. Studies indicate that T2FLS significantly surpasses T1FLS in these domains [21].

Several previous studies have applied customized PBC to control DFIG system in the literature as in [22], The authors implemented a customized PBC strategy for a DFIG system operating under time-varying load torque conditions, with the objective of accurately tracking both flow and velocity trajectories. In [23], a control approach based on IDA-PBC was presented to manage DFIG systems facing network voltage imbalance scenarios. This approach significantly enhanced the DFIG system's ability to resist and overcome various types of faults effectively. In [12], the authors used the SIDA-PBC approach for the adjustment of DFIG across various operating circumstances. The findings demonstrated exceptional sensitivity, especially with the resilience of the control system across different scenarios. In [24] The authors implemented the IDA-PBC control methodology on the DFIG system. They developed a MRAS adaptive observer designed to estimate rotor speed. The findings indicated enhanced robustness and improved accuracy in tracking WS variations. In [14], the authors proposed a control strategy combining PBC and IT2-FLC control to manage the DFIG under variable WS conditions. The results of this study also demonstrated high sensitivity and robustness.

Distinct from previous research, this paper presents a novel methodology that combines IDA-PBC with IT2-FLC by leveraging the inherent capability of IDA-PBC to manage nonlinearities effectively. This unique feature of IDA-PBC enhances the flexibility of compensation mechanisms within the system. One of the foundational concepts in IDA-PBC is the use of port control Hamiltonian (PCH) for the closed-loop (CL) regularization of nonlinear systems, which plays a critical role in stabilizing system dynamics. However, a major challenge encountered in this approach lies in accurately identifying the elements of the nonlinear forces that do not contribute to or influence the overall system dynamics [25, 26, 27]. This paper also included a comprehensive and detailed comparison with the IDA-PBC methodology. The proposed techniques were tested according to the following criteria: reference tracking at both constant and variable WS, robustness against parameter changes, and harmonic analysis (power quality assessment) to evaluate performance robustness and the efficacy of the developed approach in enhancing DFIG features. Comprehensive results from these evaluations confirm that integrating an IT2-FLC into the control scheme significantly improves power quality. It also enhances the ability to accurately track references under changing conditions and facilitates disturbance detection. The primary aims of this study are outlined below:

- Increased PFLC control durability.
- To reduce THD of the current by employing PFLC.
- To demonstrate that PFLC offers superior improvements in power quality compared to the IDA-PBC approach.
- To minimize overshoot and enhance the dynamic response

2. Methods and tools

2.1 Wind turbine system modeling

Figure 1 clearly illustrates the WECS conversion system and its main components.

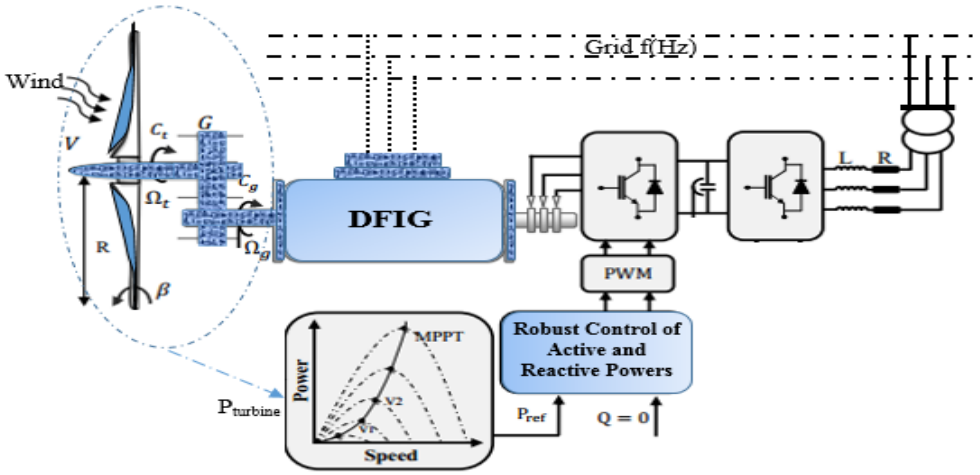

Fig 1: Generator-side control schematic.

2.1.1 Turbine model

The correlation between WS and the energy that turbines can derive from wind kinetic energy (P_m) is articulated in the subsequent equation [28,29].

$$P_m = \frac{1}{2}\rho\pi R^2 v^3 C_P \tag{1}$$

The equation connects the power coefficient C_P to the tip speed ratio λ, with R denoting the blade length and λ signifying its rotating speed.

$$\lambda = \frac{\Omega.R}{v} \tag{2}$$

The C_P can theoretically reach a maximum of 0.593 [30], while Ω indicates the angular velocity of the turbine rotor. The ratio of transferred power to rotor speed, Ω, defines turbine torque [28,29].

$$T_m = \frac{P_m}{\Omega} = \frac{1}{2\lambda}\rho\pi R^3 v^2 C_p \tag{3}$$

Equation (4) tells us what Cp is for the wind turbine system [31, 32]. When the tilt angle is 0°, Cp, which has to do with the output power, is at its highest.

$$C_p(\lambda,\beta) = \left(0.5 - 0.00167(\beta - 2)\right)\sin\left[\frac{\pi(\lambda+0.1)}{18.5-0.3(\beta-2)}\right] - 0.00184(\lambda-3)(\beta-2) \tag{4}$$

To optimize WT performance, the maximum power point tracking (MPPT) controller adjusts rotor speed while maintaining the blade pitch angle (β) at its minimal value. This strategy preserves the turbine's operation at the optimal tip-speed ratio (λ_{opt}), where the Cp reaches its peak (Cp-max) [11, 13]. The torque reference T_{m-ref} was established by [33, 34].

$$T_{m-ref} = \frac{\rho}{2}\frac{c_{p-max}}{\lambda_{opt}^3}\pi\frac{R_t^5}{G}\Omega_{mec}^2 \tag{5}$$

The pitch controller regulates the rotor blades by adjusting their angle to optimize power output at varying wind speeds [30].

2.1.2 Five–level NPC converter model (RSC)

Multilevel converters have become increasingly popular and widely used in DFIG-based WECS [35]. The five-level NPC converter topology is shown in Figure 2.

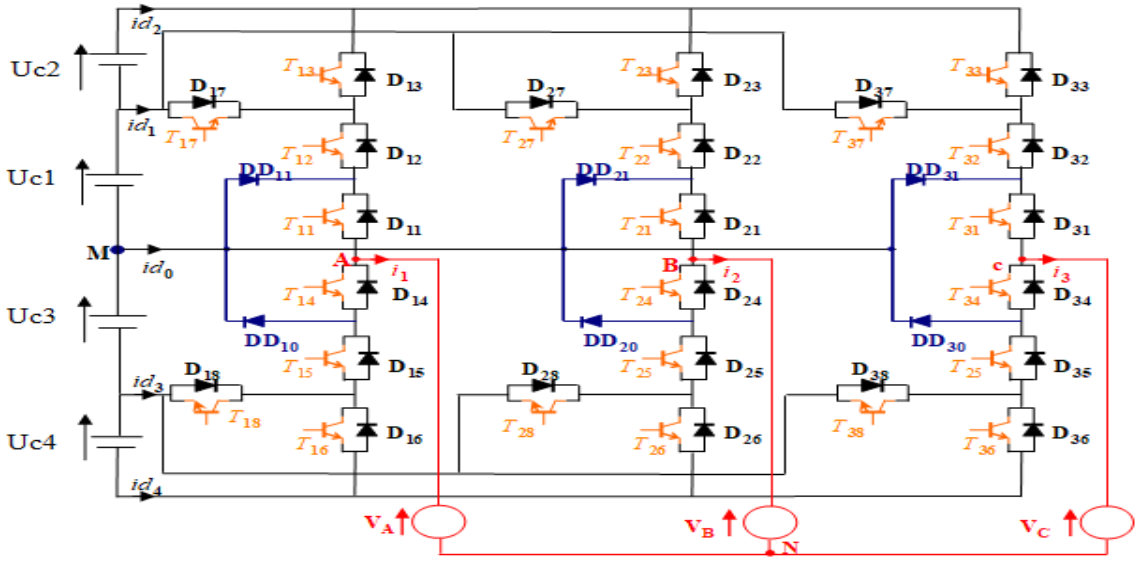

Fig 2: Topology of the five-level NPC converter.

Table 1 has been designed to facilitate a clearer and more comprehensive understanding of the switching status. According to this table, the five-level circuit operates in five different modes. corresponding to voltage levels of 2Vdc, Vdc, 0, -Vdc, and -2Vdc, determined by the switch position when activated in the auxiliary circuit.

Table 1: The state of switching for a 5-level circuit

Output Voltage	S1	S2	S3	S4	S5	S6
+2Vdc	1	1	0	0	0	1
-2Vdc	0	0	1	1	1	0
+Vdc	0	1	1	0	0	1
-Vdc	0	1	1	0	1	0
0	1	1	0	0	1	0
0	0	0	1	1	0	1

This study focuses on the implementation of the triangular-sinusoidal pulse width modulation (PWM) technique. Specifically, it achieves this by utilizing four triangular bipolar carriers to execute the modulation process effectively.

2.1.3 DFIG model

The equations that define the electrical component of the DFIG in the two-phase reference are presented by the subsequent relations [28]:

$$\begin{cases} V_{sd} = R_s I_{sd} + \frac{d\phi_{sd}}{dt} - \omega_s \phi_{sq} \\ V_{sq} = R_s I_{sq} + \frac{d\phi_{sq}}{dt} + (\omega_s - \omega)\phi_{sd} \\ V_{rd} = R_r I_{rd} + \frac{d\phi_{rd}}{dt} - \omega_s \phi_{rq} \\ V_{rq} = R_r I_{rq} + \frac{d\phi_{rq}}{dt} + (\omega_s - \omega)\phi_{rd} \end{cases} \quad (6)$$

With:

$$\begin{cases} \phi_{sd} = L_s I_{sd} + M I_{rd} \\ \phi_{sq} = L_s I_{sq} + M I_{rq} \\ \phi_{rd} = L_r I_{rd} + M I_{sd} \\ \phi_{rq} = L_r I_{rq} + M I_{sq} \end{cases} \quad (7)$$

The system mechanical equation is

$$\Gamma_{em} = \Gamma_r + C_f \Omega_{mec} + J_T \frac{d\Omega_{mec}}{dt} \quad (8)$$

A representation of torque may be found as follows:

$$\Gamma_{em} = p \frac{M}{L_s} \left(\phi_{sd} I_{rq} - \phi_{sq} I_{rd} \right) \quad (9)$$

The definitions of DFIG powers are:

$$\begin{cases} P_s = V_{sd} I_{sd} + V_{sq} I_{sq} \\ Q_s = V_{sq} I_{sd} - V_{sd} I_{sq} \end{cases} \quad (10)$$

2.2 Passivity-fuzzy logic controller

2.2.1 IDA-PBC method

Because of the DFIG's interaction with electrical currents and speed, the dynamic model is non-linear. Optimizing torque per ampere, the vector control concept eliminates the direct axis current I_d and aligns all linkage flux along the d-axis.

$$\begin{cases} \dot{\phi_{sd}} = V_{sd} - R_s I_{sd} + \omega_s L_s I_{sq} + \omega_s M I_{rq} \\ \dot{\phi_{sq}} = V_{sq} - R_s I_{sq} - \omega_s L_s I_{sd} - \omega_s M I_{rd} \\ \dot{\phi_{rd}} = V_{rd} - R_r I_{rd} + (\omega_s - \omega) L_r I_{rq} + (\omega_s - \omega) M I_{sq} \\ \dot{\phi_{rq}} = V_{rq} - R_s I_{rq} - (\omega_s - \omega) L_r I_{rd} + (\omega_s - \omega) M I_{sd} \end{cases} \quad (11)$$

The following are the state variables: $x = [\phi_s^T \phi_r^T J\omega\ ]^T = [x_e^T x_m\ ]^T$

With the variables representing the electrical state are $x_e^T = [\phi_s^T \phi_r^T]$, mechanical variable $x_m = J\omega$

Here is the expression for the energy function:

$$H(x) = \frac{1}{2} x_e^T L^{-1} x_e + \frac{1}{2 J_{DFIG}} x_m^2 \quad (12)$$

With: $L = \begin{bmatrix} L_s I_2 & M I_2 \\ M I_2 & L_r I_2 \end{bmatrix}, I_2 = \begin{bmatrix} 1 & 0 \\ 0 & 1 \end{bmatrix}$

In the context of energy and state variables, the partial derivatives are:

$$\begin{cases} \frac{\partial H}{\partial x_e} = L^{-1} x_e \\ \frac{\partial H}{\partial x_m} = J^{-1} x_m \end{cases} \Rightarrow \begin{cases} \frac{\partial H}{\partial x_e} = I = [I_s^T I_r^T]^T \\ \frac{\partial H}{\partial x_m} = \omega \end{cases} \quad (13)$$

The PCH model that describes the behavior of the DFIG is represented and formulated in the manner shown below [16].

$$\begin{cases} \dot{x} = [J(x) - R(x)]\nabla H + \mathrm{g}(x)u \\ \dot{y} = \mathrm{g}^T(x)\nabla H \end{cases} \tag{14}$$

Lastly, the matrices that represent the command, damping, and interconnection are as follows:

$$J(x) = \begin{bmatrix} -\omega_s L_s J_2 & -\omega_s M J_2 & 0_{2\times1} \\ -\omega_s L_s J_2 & -\omega_r L_s J_2 & M J_2 I_s \\ 0_{1\times2} & M I_S^T J_2 & 0 \end{bmatrix} \; R(x) = \begin{bmatrix} R_s I_2 & 0_{2\times2} & 0_{2\times1} \\ 0_{2\times2} & R_r I_2 & 0_{2\times1} \\ 0_{1\times2} & 0_{1\times2} & T_f \end{bmatrix} \tag{15}$$

$$\mathrm{g}(x) = \begin{bmatrix} I_2 & 0_{2\times2} & 0_{2\times1} \\ 0_{2\times2} & I_2 & 0_{2\times1} \\ 0_{1\times2} & 0_{1\times2} & 1 \end{bmatrix} \; u = [V_s^T \quad V_r^T \quad T_r]^T \tag{16}$$

With $0_{2\times2} = \begin{bmatrix} 0 & 0 \\ 0 & 0 \end{bmatrix}$, $0_{2\times1} = \begin{bmatrix} 0 \\ 0 \end{bmatrix}$, $0_{1\times2} = [0\ 0]$ $V_s^T = \begin{bmatrix} V_{sd} \\ V_{sq} \end{bmatrix}$ $V_r^T = \begin{bmatrix} V_{rd} \\ V_{rq} \end{bmatrix}$ $J_2 = \begin{bmatrix} 0 & -1 \\ 1 & 0 \end{bmatrix}$, $I_s = \begin{bmatrix} I_{sd} \\ I_{sq} \end{bmatrix}$, $I_r = \begin{bmatrix} I_{rd} \\ I_{rq} \end{bmatrix}$

$$J(x) = J(x)^{-1}, R(x) = R(x)^T \geq 0 \tag{17}$$

To compute the control voltages, it is necessary to ascertain $J_d(x)$ and $R_d(x)$.

To accomplish this, it is necessary to determine $J_d(x)$ and $R_d(x)$ of the controller. The CL system can be represented in the following manner:

$$f(x) + g(x)u = \big(J_d(x) - R_d(x)\big)\partial H_d(x) \tag{18}$$

Where:

$$\begin{aligned} J_d(x) &= J(x) + J_a(x) \\ R_d(x) &= R(x) + R_a(x) \\ H_d(x) &= H(x) + H_a(x) \end{aligned} \tag{19}$$

Equation (18) can be written as follows:

$$\big(J_d(x) - R_d(x)\big)\partial H_a(x) = -\big(J_a(x) - R_a(x)\big)\partial H(x) + g(x)u \tag{20}$$

Thus, the intended total energy is:

$$H_d(x) = \frac{1}{2}(x_e - x_e^*)^T L^{-1}(x_e - x_e^*) + \frac{1}{2J_{DFIG}}(x_m - x_m^*)^2 \tag{21}$$

So $$H_a(x) = H_d(x) - H(x) = -x_e^T L^{-1} x_e - \frac{1}{J_{DFIG}} x_m^* x_m + \frac{1}{2} x_e^{*T} L^{-1} x_e^* + \frac{1}{2J_{DFIG}} x_e^{*2} \tag{22}$$

With $\partial H_a(x) = \begin{bmatrix} -I^* \\ -\omega^* \end{bmatrix}$, *where* $I = [I_{sd} I_{sq} I_{rd} I_{rq}]^T$

By utilizing this relationship, (20) is converted into:

$$\big(J_d(x) - R_d(x)\big)\begin{bmatrix} -I^* \\ -\omega^* \end{bmatrix} = -\big(J_a(x) - R_a(x)\big)\begin{bmatrix} I \\ \omega \end{bmatrix} + g(x)u \tag{23}$$

In the matrix presented in (23), the command V_r is found in lines 3 and 4. Therefore:

$$J_a(x) = \begin{bmatrix} 0_{2\times2} & 0_{2\times2} & 0_{2\times1} \\ 0_{2\times2} & 0_{2\times2} & -J_{rm}(x) \\ 0_{1\times2} & J_{rm}^T(x) & 0 \end{bmatrix}, \; R_a(x) = \begin{bmatrix} 0_{2\times2} & 0_{2\times2} & 0_{2\times1} \\ 0_{2\times2} & rI_2 & 0_{2\times1} \\ 0_{1\times2} & 0_{1\times2} & 0 \end{bmatrix} \tag{24}$$

Where:

$J_{rm}^{T}(x) \in \Re^{2\times1}$to be determined, r: The extra resistance acts as a dampener for the momentary resonances produced by the currents. We use the formula (24) to find out after we substitute the matrices $J_a(x)$ and $R_a(x)$:

$$J_{rm}^{T}(x) = M\frac{(I_r - I_r^*)^T}{|I_r - I_r^*|^2}(I_s - I_s^*)^T J_2 I_r^* \tag{25}$$

So:

$$V_r = V_r^* - (\omega - \omega^*)(L_r J_2 I_r^* + J_{rm}(x)) - M\omega^* J_2(I_s - I_s^*) \ - rI_2(I_r - I_r^*) \tag{26}$$

The order is singular at the equilibrium point. The singularity can be resolved through the implementation of a variable depreciation rate. Maintaining $J_d(x)$ and $H_d(x)$ in their original state, we proceed to convert the R_a matrix into the subsequent configuration [14]:

$$R_a(x) = \begin{bmatrix} 0_{2\times2} & 0_{2\times2} & 0_{2\times1} \\ 0_{2\times2} & rI_2 & 0_{2\times1} \\ 0_{1\times2} & 0_{1\times2} & \xi(x) \end{bmatrix} \tag{27}$$

With:

$$\xi(x) = \frac{T_{em}^* - T_{em}(x_e)}{\omega - \omega^*} \tag{28}$$

And:

$$T_{em}^* = C_f \omega^* \tag{29}$$

To remove singularity, the CL Hamiltonian equation multiplies $\xi(x)$ by $(\omega - \omega^*)$. Equation (23) simply changes the mechanical aspect, therefore the formulation of V_r in terms of $J_{rm}(x)$stays constant. The equilibrium points equations allow us to infer:

$$J_{rm}(x) = MJ_2 I_s \tag{30}$$

The CL dynamic system often employs the form (14), which includes:

$$J_d(x) = \begin{bmatrix} -\omega_s L_s J_2 & -\omega_s M J_2 & 0_{2\times1} \\ -\omega_s L_s J_2 & -\omega_r L_s J_2 & MJ_2 I_s \\ 0_{1\times2} & MI_S^T J_2 & 0 \end{bmatrix};\ R_d(x) = \begin{bmatrix} R_s I_2 & 0_{2\times2} & 0_{2\times1} \\ 0_{2\times2} & (R_r + r)I_2 & 0_{2\times1} \\ 0_{1\times2} & 0_{1\times2} & T_f + \xi(x) \end{bmatrix} \tag{31}$$

And lastly, these are the order's rotor voltages.

$$V_r = V_r^* - (\omega - \omega^*)(L_r J_2 I_r^* + MJ_2 I_s) - M\omega^* J_2(I_s - I_s^*) - rI_2(I_r - I_r^*) \tag{32}$$

With:

$$V_r^* = (\omega_s - \omega^*)(L_r J_2 I_r^* + MJ_2 I_s^*) + R_r I_2 I_r^* \tag{33}$$

2.2.2 Controller type-2 fuzzy sets

Developed on Zadeh's "fuzzy fuzzy" sets idea from 1975, type 2 fuzzy sets (T2-FSs) provide a more sophisticated way to depict uncertainty [36]. Type-2 fuzzy sets (T2-FSs) have upper and lower membership functions (MF), making them more ambiguous than type-1 fuzzy sets. These functions establish an area known as the FOU to better depict imprecise data. The primary distinction between IT2-FLC and T1-FLC is in the variety of reduction procedures involved [37,38]. Figure 3 illustrates the constituents of Type-1 and Type-2 triangles. Equation (34) describes Type-1 MF:

$$A = (x, \mu_A(x)) \ | x \in X \tag{34}$$

The association degree between variable A and group x is $\mu_A(x)$, which ranges from 0 to 1. Since each x variable also ranges from 0 to 1, representing uncertainty becomes impossible. Type-2 MF should be used when the degree of participation of a variable remains uncertain and cannot be assured [37].

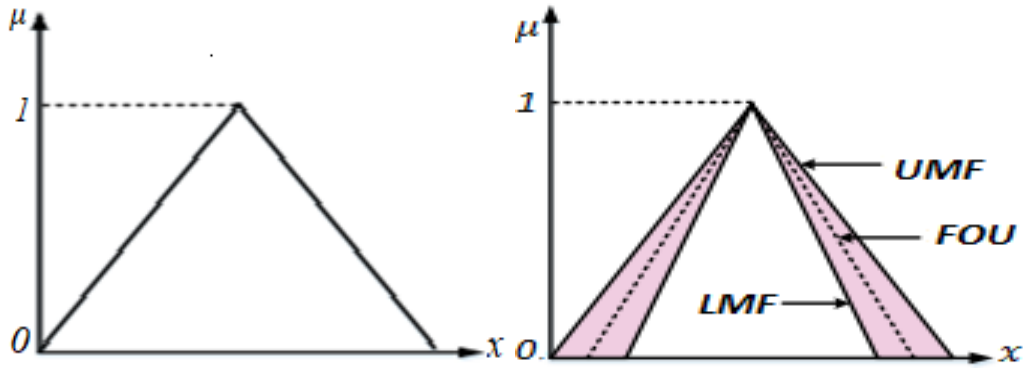

(a) **(b)**

Fig 3: MFs of the for (a) Type 1 (b) Type 2.

The equations presented below clarify the T2-FS illustrated in Figure 3 (b) and enable its representation [38]:

$$\tilde{A}=\{(x,u,(\mu_{\tilde{A}}(x,u))\}\,|\,\forall_x \epsilon X,\forall_u \epsilon J_x^u \subseteq [0,1] \quad (35)$$

$$\tilde{A}=\int_{x\in X}\int_{u\in J_x} 1/\mu_{\tilde{A}}(x,u) J_x \subseteq [0,1] \quad (36)$$

The double integral may represent all possible values of x and u when J_x is a real integer within the interval [0-1]. The amalgamation of all main memberships is referred to as the FOU. Furthermore, the FOU represents the superiority of a T2FLS and is articulated as [39,40].

$$FOU(\tilde{A}) = \cup_{\forall x\in X}\ J_x = \{(x,u); u\epsilon J_x \subseteq [0,1]\} \quad (37)$$

IT2-FLCs have a similar architecture to T1-FLCs but incorporate them within the database, necessitating type reduction to convert IT2-FLC outputs to T1-FLCs, as illustrated in Figure 04. The IT2-FLCs consist of the following components:

- The fuzzifier stage translates real-valued inputs into fuzzy ones.
- Linguistic norms convey the knowledge base, which encompasses human understanding of control issues. Logical connections transform knowledge into rule bases. The following summarizes these rules:

$$If\ e_1 is \bar{F}_1^i and\ if\ e_2\ is \bar{F}_2^i\ If\ e_n is \bar{F}_n^i\ ,\ then\ y^i = \tilde{G}^i i=1,.\ M \quad (38)$$

- An inference engine that uses the knowledge base to transform fuzzy control inputs.
- The type-2 fuzzy group can be converted into a type-1 fuzzy group using various reduction methods, such as joint center, sum center, height, etc [41,42].
- To produce understandable results, it is necessary to defuzzify the reduced Type-1 fuzzy logic system.

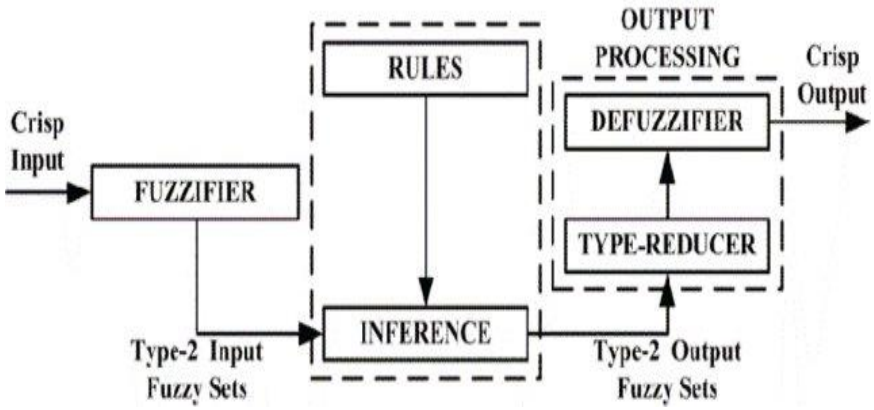

Fig 4: IT2- FLS configuration [36].

2.2.3 PFLC controller applied to DFIG

The outlined framework is structured as a two-tier loop. The outer tier uses an IT2-FLC to oversee power management. The inner tier comprises a reconfigured IDA-PBC scheme that acts as a dynamic feedback mechanism leveraging measured state variables, including rotor and stator currents and rotational speed. Figure 5 provides a depiction of the proposed control.

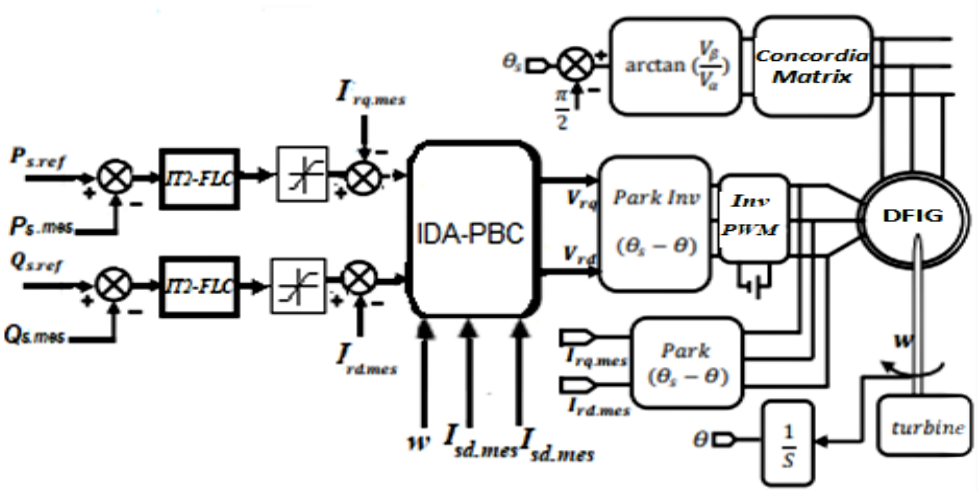

Fig 5: Structure of the control PFLC method for DFIG

Figure 6 shows the results and functions of the members. Interval [-1, 1], we find the voice input and output domains.

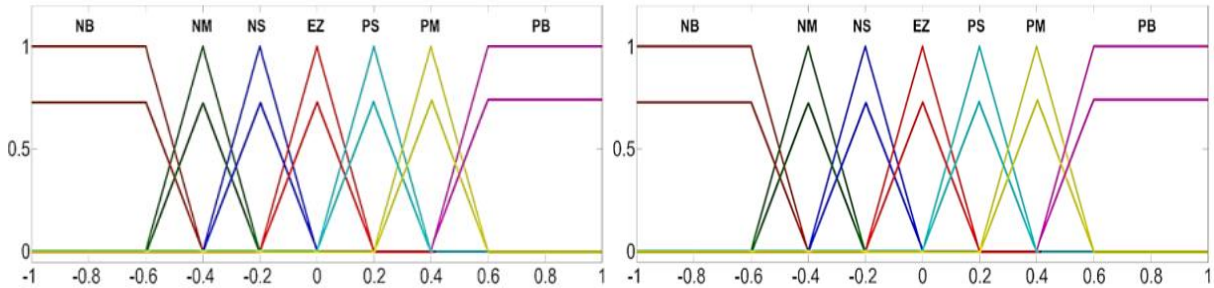

(a) **(b)**

Fig 6: MF for inputs and output.

An inference matrix is a method of presenting the aforementioned M rules. Table 2: shows one possible inference matrix for the scenario of providing seven fuzzy type-2 intervals. It sets the variables that are put into the system and the variables that are taken out of it.

Table 2: Base tables for FLC rules.

de \ *e*	NB	NM	NS	ZE	PS	PM	PB
NB	NB	NB	NB	NB	NM	NS	ZE
NM	NB	NB	NB	NM	NS	ZE	PS
NS	NB	NB	NM	NS	ZE	PS	PM
ZE	NB	NM	NS	ZE	PS	PM	PB
PS	NM	NS	ZE	PS	PM	PB	PB
PM	NS	ZE	PS	PM	PB	PB	PB
PB	EZ	PS	PM	PB	PB	PB	PB

3. Simulation results

We evaluated the efficacy of the IDA-PBC and PFLC techniques in the MATLAB environment, utilizing system parameters specified in Table 3. The controllers' performance was assessed using numerical data and graphs across three tests: a trace test, a robustness test against machine parameter variations, and disturbances from extremely high wind speeds.

Table 3: WECS parameters

Parameters	Value	Parameters	Value
P_n	10 kW	M	0.034 H
V_n	230/400 V	P	2
Rs	0.455 Ω	ρ	1.225Kg/m^3
Rr	019 Ω	R_b (Blade radius)	3.45m
Ls	0.07 H	Hm (Inertia constant)	2s
Lr	0.0213 H	D (Damping coefficients)	0.01Nm.s/rad

3.1 References tracking test at fixed wind speed

The proposed generator efficiency control methods are tested at a constant 10 m/s wind speed on turbine blades under optimal, failure-free conditions. Figure 07 shows that both IDA-PBC and PFLC effectively track active and reactive forces, with zero error in steady-state forces. Both controllers performed well, achieving perfect separation of the two stator power components.

The rotor current's quadrature component, Irq, regulates active power, while the direct component, Ird, governs the transmission of reactive energy from the stator to the grid. Figure 08 shows that the rotor currents are aligned with the reference trajectories, preventing any overshoot. The DFIG's rotor and stator currents are sinusoidal and three-phase, as depicted in Figure 9.

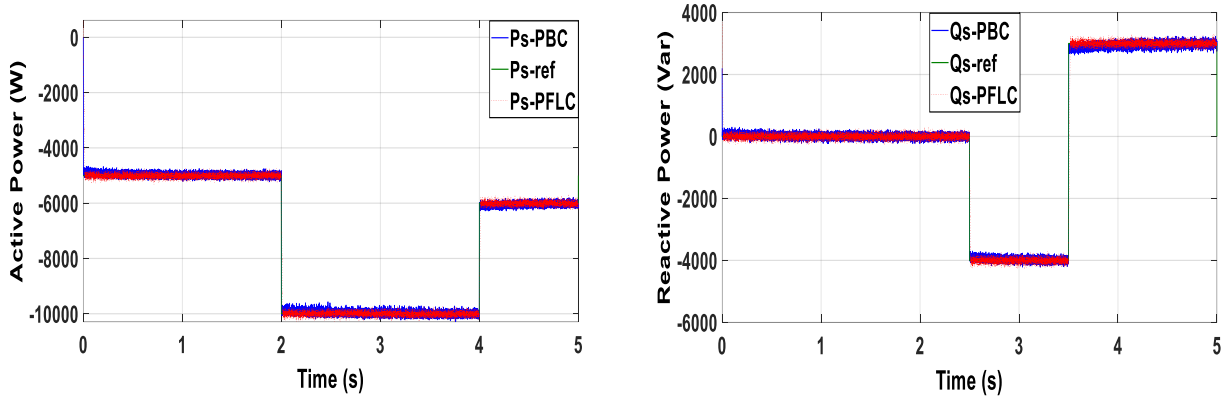

(a) **(b)**

Fig 07: DIFG power: (a) Ps and (b) Qs.

The DFIG's one-phase stator current harmonic spectrum is shown in Figure 10. This was found using the Fast Fourier Transform (FFT) for both controllers. The comparison shows that total harmonic distortion (THD) is much lower with PFLC (THD = 3.29%) than with IDA-PBC (THD = 3.59%), which means that PFLC is about 8.35% less likely to cause THD. This improvement indicates that the PFLC method offers better quality than the IDA-PBC method. The PFLC command also produced higher fundamental signal amplitude (50 Hz) than the IDA-PBC method, showing that PFLC is better than IDA-PBC.

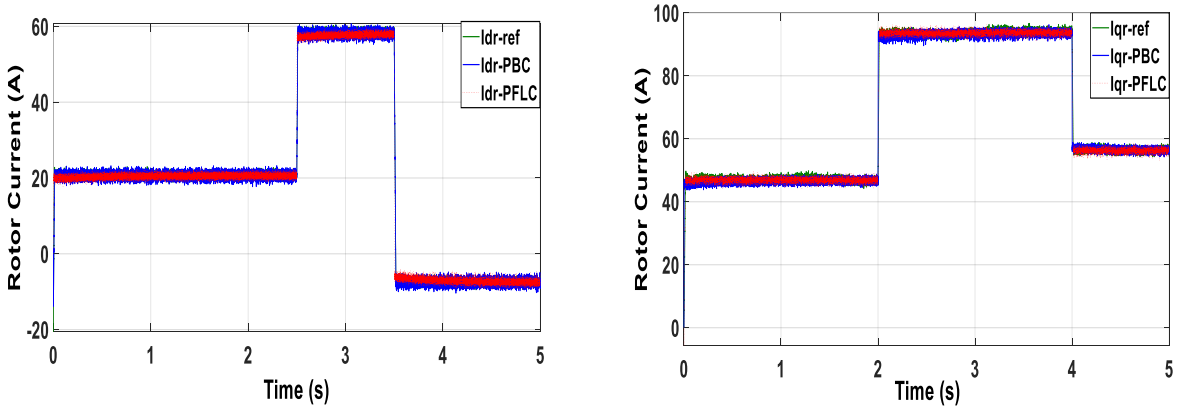

(a) **(b)**

Fig 08: Rotor current (a) Idr; (b) Iqr.

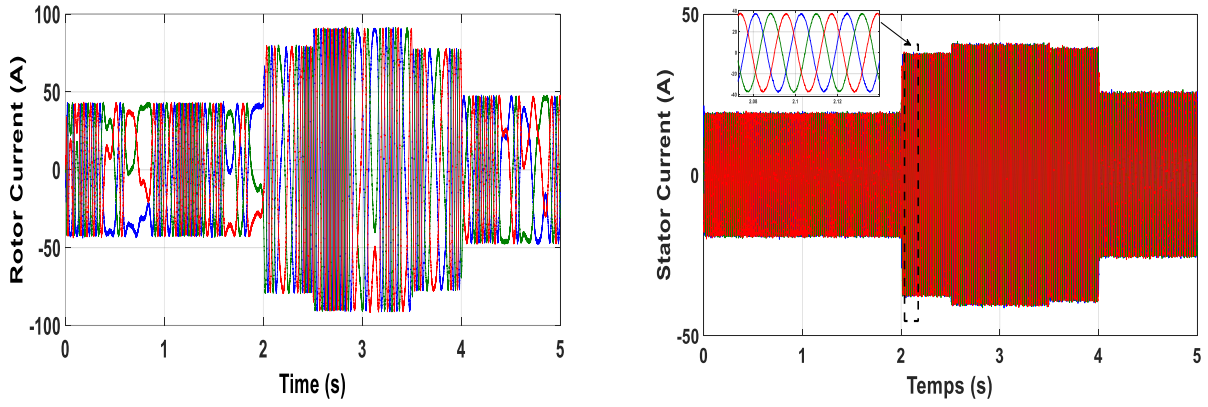

(a) **(b)**

Fig 09: (a) Rotor current; (b) stator current.

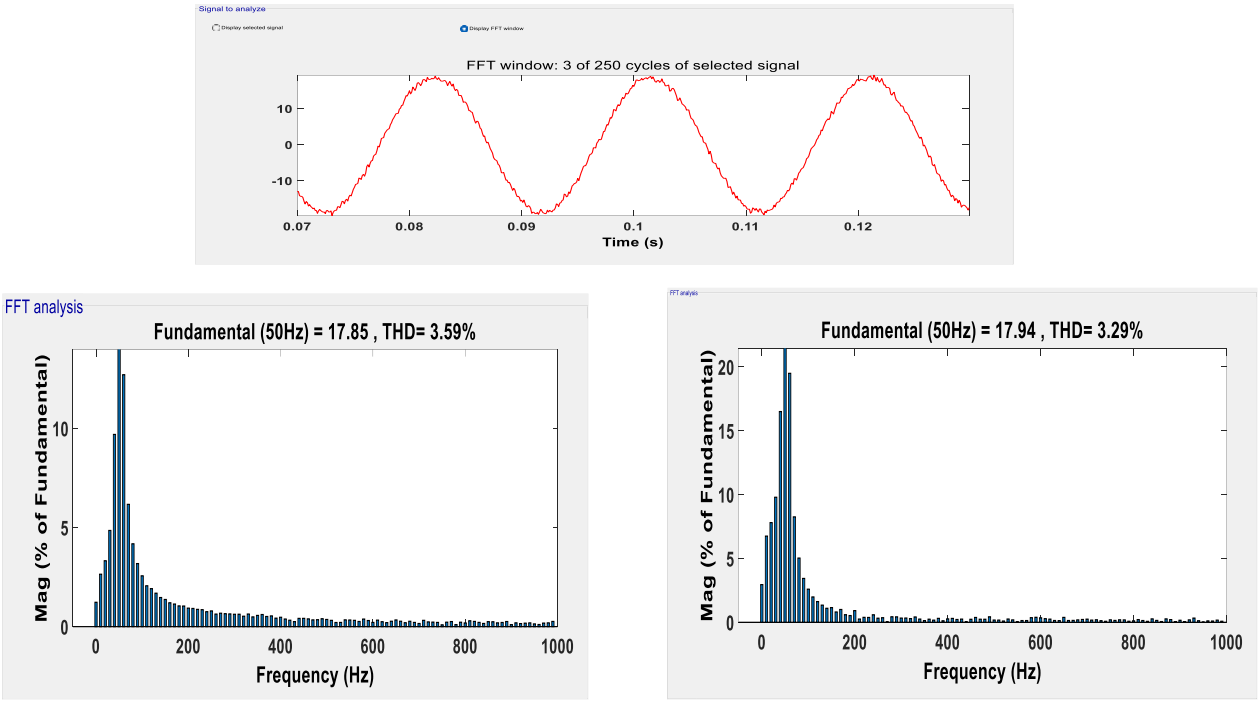

(a) **(b)**

Fig 10: (a) THD IDA-PBC; (b) THD PFLC

3.2 Robustness test against parameter variations

This part tests how well and how resilient the PFLC controller is when the control system parameters change, and then compares the results with the IDA-PBC method. The evaluation involves modifying the generator's internal characteristics to test the PFLC resilience and response time to uncertainties compared to the IDA-PBC approach. The modifications include doubling Rr and Rs, reducing Ls and Lr by 30%, and cutting M to 50%. The results, illustrated in Figure 11, demonstrate that the PFLC strategy attains superior accuracy, with Ps and Qs closely tracking their reference values. Conversely, the IDA-PBC strategy exhibits a slight overshoot at the set point, indicating greater sensitivity to parameter variations. Additionally, the PFLC controller demonstrates significantly faster response times and reduced power fluctuations compared to the IDA-PBC method. Overall, the simulations confirm that the PFLC controller is the optimal solution for achieving reliable and efficient control, as well as consistent durability, despite variations in the machine parameters.

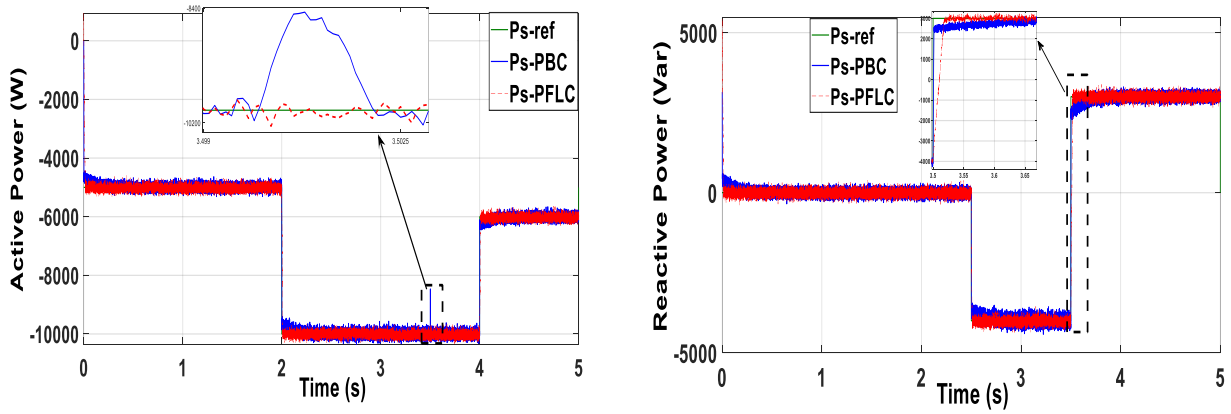

(a) **(b)**

Fig 11: DIFG power: (a) Ps and (b) Qs.

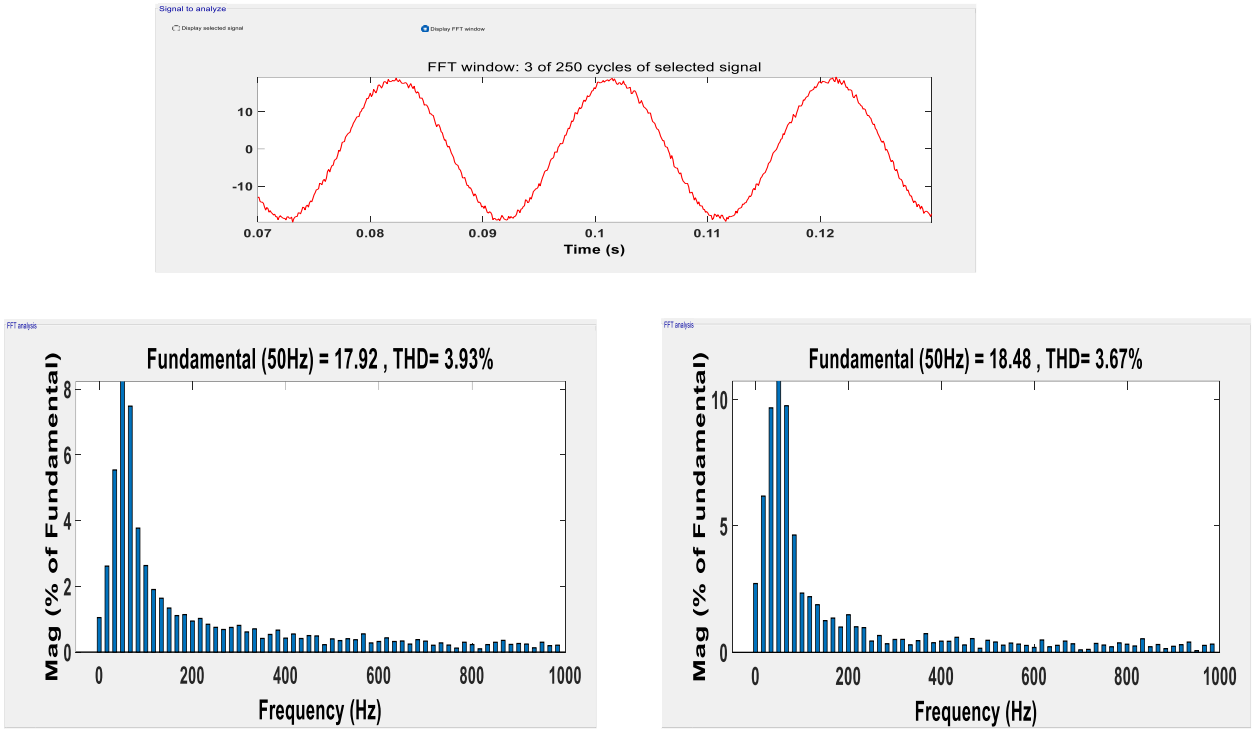

(a) **(b)**

Fig 12 : (a) THD IDA-PBC; (b) THD PFLC

Figures 12 (a) and (b) show the current THD values for different control methods. The IDA-PBC method resulted in a THD of 3.93%, while the PFLC method reduced it to 3.67%, improving current quality and decreasing ripples by 06.61% (see Table 4). The amplitude of the fundamental (50 Hz) current signal was 18.48 A with the PFLC method, compared to 17.92 A with the IDA-PBC method, indicating the superiority of the PFLC approach. Through these results, it can be said that the PFLC controller is much better than the IDA-PBC technique in many aspects as a result of using IT2-FLC.

Table 4: The current THD values between the two tests

	THD % (Test 1)	THD % (Test 2)
IDA-PBC	3.59	3.93
PFLC	3.29	3.67
Ratio	08.35%	06.61%

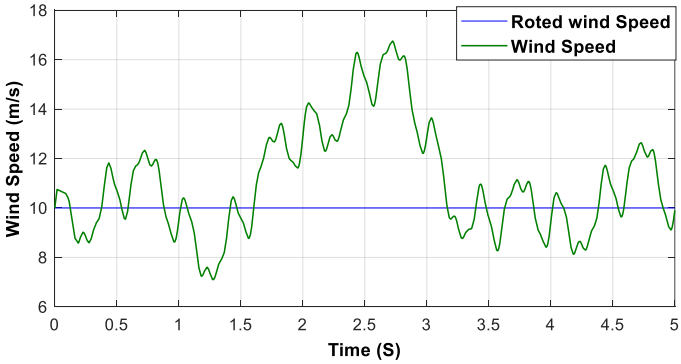

Fig 13: Wind speed

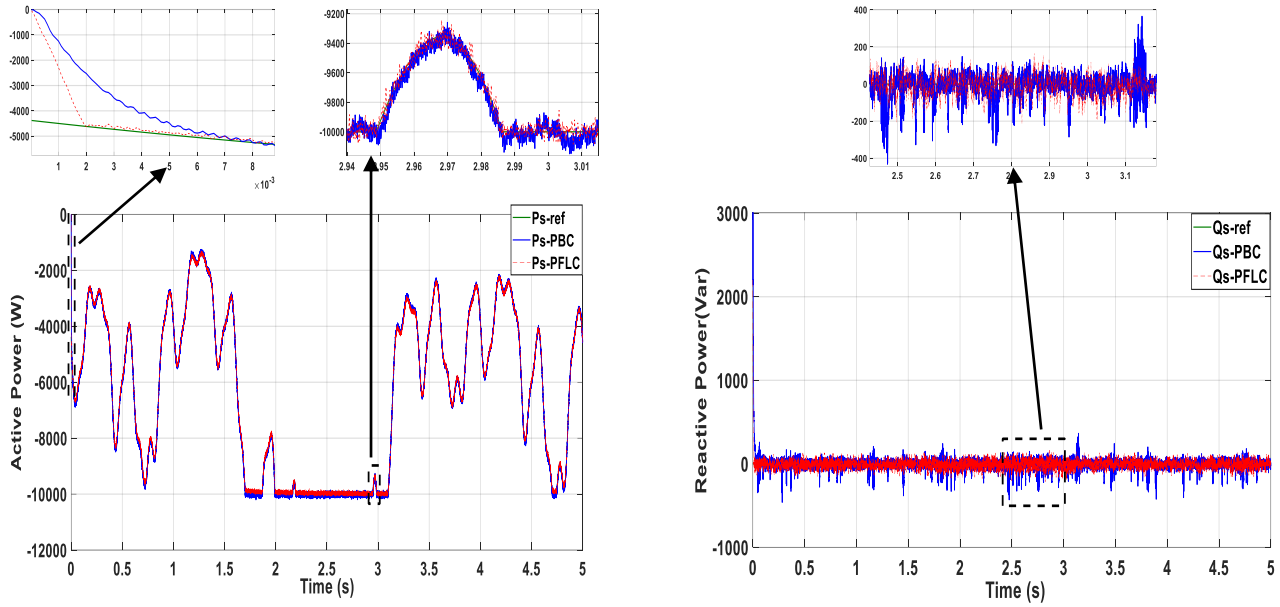

(a) **(b)**

Fig 14: DIFG power: (a) Ps and (b) Qs

3.3 References tracking test at variable wind speed

This section analyzes the tracking performance and proposes control strategies for a WT operating under an average fluctuating WS of 10 m/s. Qs is maintained at zero, while Ps generation is optimized using the MPPT method. Figure 13 shows a wind velocity. At this sub-nominal speed, the WT operates in MPPT mode, thereby generating optimal power output. When the WS exceeds the nominal value, the controller modifies the turbine's rotational speed to ensure a consistent power output during the interval [1.7 s, 3.2 s]. The negative Ps signals that the DFIG is delivering energy to the grid. The reactive power (Qs) is minimized to zero to sustain a constant power factor (PF), as illustrated in Figure 14(b). The PFLC and IDA-PBC controllers exhibited strong performance, with the PFLC demonstrating an exceptional transient response and promptly achieving the reference targets. The controllers successfully decoupled the two stator power components. Ripples were observed in Ps and Qs; however, the PFLC exhibited fewer ripples compared to the IDA-PBC.

Figure 15 shows that the three-phase voltages and currents form a balanced system. It also indicates that voltage and current are in phase opposition, confirming that Ps is delivered to the grid with a unity power factor.

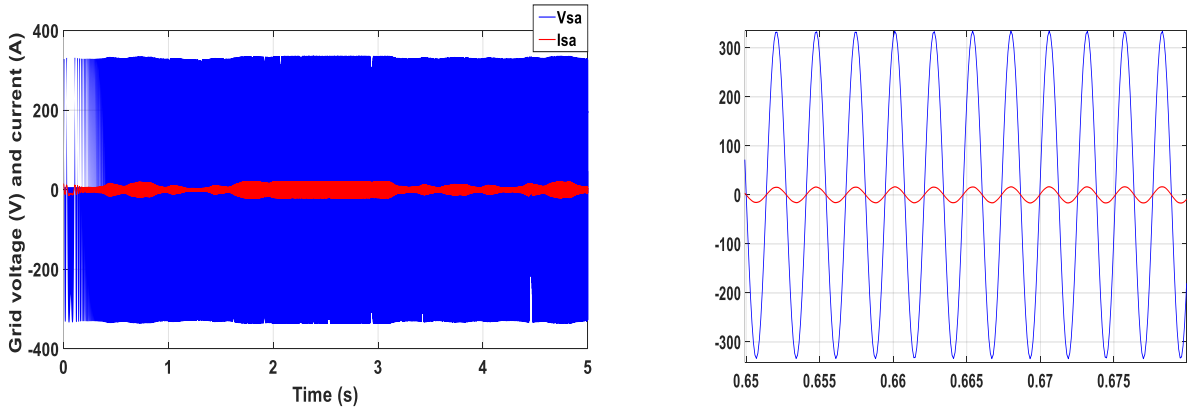

Fig 15: Grid voltage and current with a zoom

4. Conclusions

This study investigates active and reactive power management through PFLC and IDA-PBC, aiming to model, simulate, and control a system that converts wind energy into electrical energy. A hybrid passive approach combined with fuzzy control in MATLAB will be employed to compare results with IDA-PBC-based control. The focus is on a 10 kW DFIG system, assessing its resilience against variations in system parameters and disruptions caused by extremely high wind speeds. A comparison of the PFLC and IDA-PBC methods shows that PFLC is more effective, offering faster tracking and reducing error, overshoot and ripple in reactive and active power. PFLC also improves power quality and dynamic response more effectively than IDA-PBC. Although changes in system parameters impact current quality, as reflected in current THD variations, this effect is less pronounced with PFLC than with IDA-PBC. Introducing fuzzy logic into the control system improves the energetic electricity and the reactive electricity by enhancing reference tracking, sensitivity to disturbances, and resilience to parameter changes. Future studies will focus on robust controllers. We are developing a smart hybrid controller to manage a variable-speed WT with a DFIG, combining IT2-FLC and a backstepping control method.

References

[1] Xiong, L., Li, J., Li, P., Huang, S., Wang, Z., & Wang, J. "Event triggered prescribed time convergence sliding mode control of DFIG with disturbance rejection capability". *International Journal of Electrical Power & Energy Systems*, vol. 131, p. 106970, 2021. https://doi.org/10.1016/j.ijepes.2021.106970.

[2] Mousavi, Y., Bevan, G., Kucukdemiral, I. B., & Fekih, A. "Sliding mode control of wind energy conversion systems: Trends and applications". *Renewable and Sustainable Energy Reviews*, vol. 167, pp. 112734, 2022. https://doi.org/10.1016/j.rser.2022.112734

[3] Fridi, S. K., Koondhar, M. A., Jamali, M. I., Alaas, Z. M., Alsharif, M. H., Kim, M. K., ... & Ahmed, M. M. R. "Winds of **progress :**an in-depth exploration of offshore, floating, and onshore wind turbines as cornerstones for sustainable energy generation and environmental stewardship." *IEEE Access* ,vol.12, pp. 66147-66166, 2024. https://doi.org/10.1109/ACCESS.2024.3397243

[4] GWEC. Global Wind Report 2024. "Global Wind Energy Council". 2024.

[5] Sreenivasulu, Panisetty, and Jakeer Hussain. "Protection of rotor side converter of doubly fed induction generator-based wind energy conversion system under symmetrical grid voltage fluctuations." *Frontiers in Energy Research* vol.12,pp. 1465167, 2024. https://doi.org/10.3389/fenrg.2024.1465167

[6] Khan, D., Ahmed Ansari, J., Aziz Khan, S., & Abrar, U." Power optimization control scheme for doubly fed induction generator used in wind turbine generators". *Inventions*, , vol. 5, no. 3, p. 40, 2020.https://doi.org/10.3390/inventions5030040

[7] Benbouhenni, H., Bizon, N., Mosaad, M. I., Colak, I., Djilali, A. B., & Gasmi, H. "Enhancement of the power quality of DFIG-based dual-rotor wind turbine systems using fractional order fuzzy controller". *Expert Systems with Applications*, Vol. 238, pp. 121695, 2024. https://doi.org/10.1016/j.eswa.2023.121695

[8] HERIZI, Abdelghafour et ROUABHI, Riyadh. "Hybrid Control Using Sliding Mode Control with Interval Type-2 Fuzzy Controller of a Doubly Fed Induction Generator for Wind Energy Conversion". *International Journal of Intelligent Engineering & Systems*, vol.15, no.1, pp.549-562, 2022. https://doi: 10.22266/ijies2022.0228.50

[9] Kaloi, G. S., Baloch, M. H., Kumar, M., Soomro, D. M., Chauhdary, S. T., Memon, A. A., & Ishak, D." An LVRT scheme for grid-connected DFIG based WECS using state feedback linearization control technique". *Electronics*, vol.8, no.7, pp. 777,2019 .https://doi.org/10.3390/electronics8070777

[10] Itouchene, H., Amrane, F., Boudries, Z., Mekhilef, S., Benbouhenni, H., & Bizon, N. "Enhancing the performance of grid-connected DFIG systems using prescribed convergence law". *Scientific Reports*, vol.*15*,no.1, pp.28550, 2025. https://doi.org/10.1038/s41598-025-13847-x.

[11] Amira, L., Tahar, B., & Abdelkrim, M. "Sliding mode control of doubly-fed induction generator in wind energy conversion system". In: 2020 8th International Conference on Smart Grid (icSmartGrid). IEEE, 2020. pp. 96-100. https://doi: 10.1109/icSmartGrid49881.2020.9144778

[12] Hichem, H., Abderrazak, T. A., Iliace, A., Bendelhoum, M. S., & Abdelkrim, B." A new robust SIDA-PBC approach to control a DFIG". *Bulletin of Electrical Engineering and Informatics*, vol.12, no.3, pp. 1310-1317,2023. https://doi.org/10.11591/eei.v12i3.2155

[13] HEMEYINE, Ahmed Vall, ABBOU, Ahmed, TIDJANI, Naoual, *et al.* "Robust takagi sugeno fuzzy models control for a variable speed wind turbine based a DFI-generator". *International Journal of Intelligent Engineering and Systems*, vol.13, no 3, pp. 90-100,2020.https:doi: 10.22266/ijies2020.0630.09

[14] ALLALI, Izzeddine and DEHIBA, Boubekeur. "Passivity Based Control of Doubly Fed Induction Generator Using an Interval Type-2 Fuzzy Logic Controller". *The Journal of Engineering and Exact Sciences*, vol. 10, no 9, pp. 21012-21012, 2024. https: Doi: 10.18540/jcecvl10iss9pp21012

[15] Ortega, R., & Sira-Ramírez, H. " Lagrangian modeling and control of switch regulated DC-to-DC power converters". In Control Using Logic-Based Switching , *Berlin, Heidelberg: Springer Berlin Heidelberg*,2005, pp. 151-161. https://doi.org/10.1007/BFb0036092

[16] ORTEGA, Romeo et GARCIA-CANSECO, Eloisa. Interconnection and damping assignment passivity-based control: A survey. European Journal of control, vol. 10, no 5, pp. 432-450, 2004. https://doi.org/10.3166/ejc.10.432-450

[17] Minka, I., Essadki, A., Mensou, S., & Nasser, T. (2019)." Primary frequency control applied to the wind turbine based on the DFIG controlled by the ADRC". *International Journal of Power Electronics and Drive System*, vol. 10, no. 2, p. 1049-1058,2019.https:doi: 10.11591/ijpeds.v10.i2

[18] Abbas, A. K., Al Mashhadany, Y., Hameed, M. J., & Algburi, S. "Review of intelligent control systems with robotics". *Indonesian Journal of Electrical Engineering and Informatics (IJEEI)*, vol.*10*, no.4, pp.734-753,2022. https://doi.org/10.52549/ijeei.v10i4.3628

[19] Kheir Saadaoui, B. B., Assas, O., & Khodja, M. A. KHODJA, Mohammed Abdallah. "Type-1 and type-2 fuzzy sets to control a nonlinear dynamic system". *Revue d'Intelligence Artificielle*, vol. 33, no. 1, pp. 1-7,2019. https://doi.org/10.18280/ria.330101

[20] Acikgoz, H., Kececioglu, O., Gani, A., Tekin, M., & Sekkeli, M. "Robust control of shunt active power filter using interval type-2 fuzzy logic controller for power quality improvement". *Tehnicki Vjesnik-Technical Gazette*, vol24, 2017. https://doi.org/10.17559/TV-20161213004749

[21] Yan, S. R., Dai, Y., Shakibjoo, A. D., Zhu, L., Taghizadeh, S., Ghaderpour, E., & Mohammad zadeh," A fractional-order multiple-model type-2 fuzzy control for interconnected power systems incorporating renewable energies and demand response". *Energy Reports*, vol.12, pp. 187-196,2024 .https://doi.org/10.1016/j.egyr.2024.06.018

[22]WU, Wen Jun et XUE, Hua. Passivity-based control strategies of doubly fed induction wind power generator without speed sensors. *Applied Mechanics and Materials*, vol. 380, pp. 3124-3128, 2013. https://doi.org/10.4028/www.scientific.net/AMM.380-384.3124

[23]HUANG, Jiawei, WANG, Honghua, et WANG, Chong. Passivity-based control of a doubly fed induction generator system under unbalanced grid voltage conditions. *Energies*, vol. 10, no 8, pp. 1139, 2017. https://doi.org/10.3390/en10081139

[24] HICHEM, Hamiani, ABDELLAH, Mansouri, ABDERRAZAK, Tadjeddine Ali, *et al.* A wind turbine sensorless automatic control systems, analysis, modelling and development of IDA-PBC method. *International Journal of Power Electronics and Drive Systems*, vol. 11, no 1, pp. 45, 2020. https://doi.org/http://doi.org/10.11591/ijpeds.v11.i1.pp45-55

[25] Brogliato, B., Lozano, R., Maschke, B., Egeland, O., Brogliato, B., Lozano, R., ... & Egeland, O." Passivity-based control. Dissipative systems analysis and control: Theory and applications", Cham: Springer International Publishing, pp. 491-573, 2019. https://doi.org/10.1007/978-3-030-19420-8_7

[26] Yang, B., Yu, T., Shu, H., Zhang, Y., Chen, J., Sang, Y., & Jiang, L. "Passivity-based sliding-mode control design for optimal power extraction of a PMSG based variable speed wind turbine". Renewable energy, vol. 119, p. 577-589, 2018.https://doi.org/10.1016/j.renene.2017.12.047

[27] Belkhier, Y., Achour, A., Bures, M., Ullah, N., Bajaj, M., Zawbaa, H. M., & Kamel, S. "Interconnection and damping assignment passivity-based non-linear observer control for efficiency maximization of permanent magnet synchronous motor". *Energy Reports*, vol. 8, pp. 1350-1361. 2022, https://doi.org/10.1016/j.egyr.2021.12.057

[28] Sahri, Y., Tamalouzt, S., Lalouni Belaid, S., Bacha, S., Ullah, N., Ahamdi, A. A. A., & Alzaed, A. N. "Advanced fuzzy 12 dtc control of doubly fed induction generator for optimal power extraction in wind turbine system under random wind conditions". *Sustainability*, vol.13, no.21, pp. 11593, 2021.https://doi.org/10.3390/su132111593

[29] Oualah, O., Kerdoun, D., et Boumassata, A." Super-twisting sliding mode control for brushless doubly fed reluctance generator based on wind energy conversion system". *Electrical Engineering & Electromechanics*, vol.2, pp. 86-92, 2023. https://doi.org/10.20998/2074-272X.2023.2.13

[30] Adeyanju, A. A. "The Influence of Rotor Separation on The Performance of a Dual-Rotor Wind Turbine". *Journal of Namibian Studies: History Politics Culture*, vol. 35, pp. 4684-4702, 2023. https://doi.org/10.59670/jns.v35i.4573

[31] Carpintero-Renteria, M., Santos-Martin, D., Lent, A., & Ramos, C, Wind turbine power coefficient models based on neural networks and polynomial fitting., IET Renewable Power Generation, vol.14,no. 11 ,pp. 1841-1849, 2020. https://doi.org/10.1049/iet-rpg.2019.1162

[32] Castillo, OC, Andrade, VR, Rivas, JJR, & González, RO., Comparison of power coefficients in wind turbines considering the tip speed ratio and blade pitch angle., *Energies* , vol.16,no.6 ,pp2774, 2023. https://doi.org/10.3390/en16062774

[33] Mousa, H. H., Youssef, A. R., & Mohamed, E. E. "Hybrid and adaptive sectors P&O MPPT algorithm-based wind generation system". *Renewable Energy*, vol.145, pp. 1412-1429,2020. https://doi.org/10.1016/j.renene.2019.06.078

[34] Kadri, A., Marzougui, H., Aouiti, A., & Bacha, F., Energy management and control strategy for a DFIG wind turbine/fuel cell hybrid system with super capacitor storage system, Energy, 192,pp 116518, 2020. https://doi.org/10.1016/j.energy.2019.116518

[35] Cherifi, Djamila, Yahia Miloud, and Mohamed Mostefai. "Performance of Neutral Point Clamped Five Level Inverter Using Space Vector Modulation Control Fed by DPC-VF-SVM Rectifier." *WSEAS Transactions on Power Systems, vol.* 16 ,pp. 275-287,2021. https://doi.org/ 10.37394/232016.2021.16.28

[36]Wu, D., & Mendel, J. M. "Recommendations on designing practical interval type-2 fuzzy systems". *Engineering Applications of Artificial Intelligence*, vol.85, pp. 182-193, 2019. https://doi.org/10.1016/j.engappai.2019.06.012

[37] Liang, Q., & Mendel, J. M." Interval type-2 fuzzy logic systems: theory and design". *IEEE Transactions on Fuzzy systems*, vol.8, no.5, p. 535-550,2000. https://doi: 10.1109/91.873577

[38] Milles, A., Merabet, E., Benbouhenni, H., Debdouche, N., & Colak, I. " Robust control technique for wind turbine system with interval type-2 fuzzy strategy on a dual star induction generator". *Energy Reports*,vol.11, pp. 2715-2736,2024. https://doi.org/10.1016/j.egyr.2024.01.060

[39] Li, K., Zhang, X., & Han, Y. "Robot path planning based on interval type-2 fuzzy controller optimized by an improved Aquila optimization algorithm". *IEEE Access*, 2023. https://doi: 10.1109/ACCESS.2023.3323437

[40]Magaji, N., Mustafa, M. W. B., Lawan, A. U., Tukur, A., Abdullahi, I., & Marwan, M. "Application of Type 2 Fuzzy for Maximum Power Point Tracker for Photovoltaic System". *Processes*, vol. 10, no.8, pp. 1530, 2022. https://doi.org/10.3390/pr10081530

[41] Chen, C., Wu, D., Garibaldi, J. M., John, R. I., Twycross, J., & Mendel, J. M. "Comprehensive study of the efficiency of type-reduction algorithms". *IEEE Transactions on Fuzzy Systems*, vol.29,no. 6, pp. 1556-1566,2020. https://doi: 10.1109/TFUZZ.2020.2981002

[42] LATHAMAHESWARI, M., NAGARAJAN, D., KAVIKUMAR, J., et al. "Triangular interval type-2 fuzzy soft set and its application". *Complex & Intelligent Systems*, vol.6, pp. 531-544,2020. https://doi.org/10.1007/s40747-020-00151-6